Gastric Cancer (2024) 27:1078–1087
https://doi.org/10.1007/s10120-024-01525-2

ORIGINAL ARTICLE

A mathematical simulation model to determine the optimal endoscopic screening strategy for detection of *H. pylori*-naïve gastric neoplasms

Fumiaki Ishibashi[1] · Kosuke Okusa[2] · Yoshitaka Tokai[3] · Toshiaki Hirasawa[3] · Tomohiro Kawakami[4] · Kentaro Mochida[1,4] · Yuka Yanai[5] · Chizu Yokoi[5] · Yuko Hayashi[6] · Shun-ichiro Ozawa[7] · Koji Uraushihara[8] · Yohei Minato[9] · Hiroyuki Nakanishi[10] · Hiroya Ueyama[11] · Mikinori Kataoka[12] · Yuzo Toyama[13] · Yuji Mizokami[14] · Sho Suzuki[1]

Received: 3 May 2024 / Accepted: 16 June 2024 / Published online: 27 June 2024

Abstract

Background The effectiveness of esophagogastroduodenoscopy (EGD) screening in cohorts with low *Helicobacter pylori* prevalence is unknown. This study aimed to develop an optimally efficient EGD screening strategy for detecting *H. pylori*-naïve gastric neoplasms (HpNGNs).

Methods EGD data of 12 institutions from 2016 to 2022 were retrospectively analyzed. Age-related HpNGN prevalence, tumor growth rate, missing rate, and detection threshold size were calculated from the databases. Subsequently, using clinical data, a novel mathematical model that simultaneously simulated demographic changes and HpNGN detection was developed. Screening strategies using different starting ages (40/45/50 years) and intervals (2/5/10 years) were also compared. The detection rates of all tumors occurring within the virtual cohort and number-needed-to-test (NNT) were measured as outcomes.

Results Data of 519,368 EGDs and 97 HpNGNs (34 pure signet ring cell carcinomas, 26 gastric adenocarcinomas of the fundic gland type, 30 foveolar gastric adenoma-Raspberry type, and seven undifferentiated-type cancer cases) were analyzed. A virtual cohort with a 70-year time horizon was used to simulate the occurrence, growth, and detection of 346,5836 people. Among the strategies with detection rate > 50%, the screening strategy with a 5-year interval starting at 45 years of age had the lowest NNT. Adopting this strategy, most HpNGNs were detected at < 20 mm in size, and the deep submucosal invasion rate was less than 30%.

Conclusions A mathematical simulation model revealed that screening every 5 years starting at 45 years of age could efficiently assist in identifying HpNGNs at an early stage.

Keywords Early detection of cancer · Stomach neoplasms · Endoscopy · *Helicobacter pylori* · Mass screening

Introduction

Helicobacter pylori (H. pylori) infection has been shown to be related to gastric cancer (GC) development [1–4]. Since *H. pylori* infection rates in East Asia, including Japan, have been high over the previous decades [5, 6], most GCs occurring in *H. pylori*-infected mucosa are categorized as *H. pylori*-related gastric cancers (HpRGCs) [7]. HpRGC often leads to fatal outcomes via metastasis. Therefore, controlling *H. pylori* infection rates as a public health issue is important [8]. Although the recent decline in *H. pylori* infection rates has reduced the number of newly diagnosed HpRGC cases, it has also led to the growing emergence of *H. pylori*-naïve gastric neoplasms (HpNGNs) [7, 9–12].

HpNGNs are classified into several subtypes based on their origin and differentiation patterns. Gastric adenocarcinoma of the fundic gland type (GA-FG) is characterized by subepithelial tumor-like neoplasms with whitish–yellowish color showing the presence of dilated vessels on the surface [13–16]. This appearance is explained by the pattern of differentiation: the cells constituting GA-FG differentiate toward the chief cell-predominant fundic gland [13]. Foveolar-type gastric adenoma (FGA) shows two types of endoscopic findings: a small reddish elevated lesion with a

Extended author information available on the last page of the article

raspberry-like appearance (FGA-raspberry type) and a whitish flat elevated lesion (FGA-flat type) [17, 18].

Undifferentiated-type GC may also appear in *H. pylori*-uninfected mucosa. Pure signet ring cell carcinoma (PSRCC) is characterized by a small, flat, and whitish lesion in the middle and lower parts of the stomach [19]. Impaired cadherin function caused by CDH1 somatic mutation is considered a driver of PSRCC development [20–22]. PSRCC is also frequently observed in patients with hereditary diffuse GC due to germline mutations in CDH1 [23]. However, poorly differentiated GC is found only in *H. pylori*-naïve patients; it shows high malignant potential for downward invasion and lymph node metastasis [9, 24].

In future, in Japan, where HpNGNs may replace HpRGCs as the primary target for detection, screening strategies with esophagogastroduodenoscopy (EGD) will need to be changed. However, the optimal EGD screening strategy for *H. pylori*-naïve individuals remains unknown. This study aimed to develop an EGD-based screening strategy for efficiently detecting HpNGNs regarding screening efficiency.

Methods

Study design

This study comprised two phases: clinical data collection and analysis, followed by simulation model development. The study protocol was approved by the Ethics Committee of the International University of Health and Welfare (approval number: 22-Ic-009) on February 23, 2023. The requirement for written informed consent was waived due to the retrospective nature of the study. The study plan was publicized by posting the study protocol at each institution and on the website. Patients who did not wish to participate were excluded. This study was conducted according to the guidelines of the Declaration of Helsinki.

Clinical data collection phase

Data collection

Data on EGD screening examinations performed during health checkups at 12 institutions in Japan between January 2016 and December 2022 were retrospectively collected. The inclusion criteria were individuals who underwent EGD for health checkups during the period. HpNGN cases detected at the institutions were enrolled for evaluating HpNGN. The exclusion criteria encompassed cases: whose names were registered in the endoscopic database without stored images; having no evidence that the EGD was performed; wherein the report was incomplete, wherein the screening was not accomplished due to incomplete examination; and wherein HpNGN was suspected by endoscopic diagnosis without establishing pathological diagnosis. Moreover, cases diagnosed with HpNGN at another institution and referred to that institution for further examination, with missing data on the final pathology diagnosis, with a history of eradication, wherein more than one test for *H. pylori* infection status was not performed, and with pathologically proven background mucosal atrophy were excluded from the HpNGN assessment. If the same patient underwent EGD several times over the year, the data were collected as separate EGD for each.

Age and sex of individuals who underwent EGD were investigated. Additionally, detailed information on the identified HpNGNs was collected, including patient age, sex, test results for *H. pylori* infection status, final pathological diagnosis, lesion size, lesion depth, lymphovascular invasion, presence of lymph node metastasis, and EGD images. The EGD examination at the time of HpNGN diagnosis was registered as the index EGD (IE); the lesion site images were registered (Supplementary Fig. 1). If the same patient underwent EGD examinations in the past, the previous EGD images were defined as the reference EGD (RE). The RE was followed up retrospectively until the lesions noted in the IE were unrecognizable on the images. This study used each facility's own EGD database. Each endoscopist responsible for EGD at the facility entered the information into the database. The principal investigator at each facility collected information on HpNGN-detected cases by reviewing the medical records, entering the information into a case report file. Therefore, the data were sent to the data center of the International University of Health and Welfare Ichikawa Hospital.

Definition of HpNGN

HpNGN was defined as a gastric neoplasm that occurred in a patient who met all the following criteria: (1) no history of *H. pylori* eradication, (2) no mucosal atrophy on endoscopic examination, (3) no pathological mucosal atrophy, and (4) *H. pylori*-negative results using various tests for *H. pylori* infection status. The histopathological types of HpNGN were broadly classified as PSRCC, GA-FG, FGA-raspberry type, FGA-flat type, undifferentiated, and differentiated. The undifferentiated type was defined as a poorly differentiated carcinoma other than PSRCC. All detected HpNGNs were confirmed by pathological diagnoses of specimens obtained by endoscopic or surgical resection. The depth of cancer invasion was defined according to the Japanese Classification of Gastric Carcinoma [25].

Clinical data analysis for model construction

The numbers of EGDs performed per generation (E_n) and HpNGNs according to age distribution (C_n) were used to calculate the age-related prevalence of HpNGN (P_n).

$$P_n = \frac{C_n}{E_n}(1 \le n \le 7)$$

where n indicated the age group classification. The seven age groups were 20–29, 30–39, 40–49, 50–59, 60–69, 70–79, and ≥ 80 years.

The estimated tumor growth speed (X_t (mm/year)) was calculated as the difference in lesion diameter x (mm) divided by the interval y_r (year) between RE_x and IE:

$$X_t = \frac{x}{y_r}$$

where x indicated the number of previous EGDs starting from IE (Supplementary Fig. 1). If the target lesion could be recognized in all previously registered images, X_t was calculated based on the oldest endoscopic image among the registered images. Furthermore, if the interval between RE_x and RE_{x-1} was more than 5 years, X_t was calculated based on RE_{x-1}. The cases used for calculating tumor growth speed were limited to those wherein previous endoscopy had captured the area where the tumor should have been present. The detection threshold size (X_{th}) was set at 0.8 times the average tumor diameter at detection time; the missing rate (M_r) was calculated based on the number of cases without description about the lesion on the RE reports. The lesion size in RE_x or RE_{x-1} was measured by referring to the pathological final diagnosis by two endoscopists (FI and KM) in the data center.

HpNGN cases wherein the growth process could be traced were used to estimate the probability of deep submucosal (SM) invasion. Regarding each histopathological type, the intercept (a) and regression coefficient (b) were obtained by logistic regression analysis using the time from tumor occurrence to resection as the explanatory variable and the depth of resected lesions (intramucosal and shallow SM invasive carcinoma or deep SM invasive carcinoma) as the objective variable. The formula for predicting deep SM invasion (S_x) X years after the occurrence of HpNGN was:

$$S_x = a + bx$$

where S_x greater than 1 was considered to indicate deep SM invasion. Finally, the coefficients were determined such that the linear model best fit tumor size and depth in the observed data.

Simulation model development phase

Baseline setting for model construction

The following premise was set for model construction. First, the tumor growth speed (X_t) was constant. Second, the detection rate of HpNGNs was determined using a probabilistic curve defined by tumor size. The probabilistic curve was directly affected by detection threshold size (X_{th}) and missing rate (M_r). Third, the deep SM invasion rate (S_x) was affected only by the time elapsed since lesion occurrence. Fourth, demographic parameters, including fertility rate and mortality, were calculated based on Japanese population statistics. Fifth, the detected HpNGNs were eliminated at detection time, and the prevalence (P_n) in that generation was variable. The variables used in the simulation model are listed in Table 1.

Mathematical simulation model

Based on this premise and variables, a mathematical simulation model for HpNGN detection was developed. The model allowed for the simultaneous analysis of two layers: one to simulate demographic transitions and the other to simulate tumor occurrence, growth, and detection (Fig. 1). Regarding the demographic simulation layer, 100,000 people were

Table 1 Variables used in the simulation model

	PSRCC	GA-FG	FGA-raspberry type	Undifferentiated-type
Population by generation (P_g) (persons)	Calculated based on Supplementary Fig. 2			
Prevalence of HpNGN by generation (P_n) (persons/year)	Defined in Supplementary Table 1			
Mortality by generation (persons/year)	Defined in Supplementary Fig. 3			
Estimated average tumor growth speed (X_t) (mm/year)	2.5	2.7	1.2	11.3
Threshold size of the detection of HpNGN (X_{th}) (mm)	6.7	8.2	3.6	15.6
Maximum tumor size (X_m) (mm)	16	26	8	56
Missing rate (M_r) (persons/year)	0.461	0.652	0.565	0.17
Screening interval (years)	2, 5, 10 years			
Year of start of screening (year)	40, 45, 50 years old			
Year of end of screening (year)	70 years old			

PSRCC pure signet ring cell carcinoma, *GA-FG* gastric adenocarcinoma of the fundic gland type, *FGA* foveolar gastric adenoma, *HpNGN H. pylori*-naïve gastric neoplasm

born in the first year of the cohort, followed by annual births and deaths according to predefined demographic parameters; population changes were tracked for 70 years (Supplementary Figs. 2, 3). Considering the tumor analysis layer, HpNGNs occurred with a constant probability (P_n) in each generation. The number of generated tumors constantly increased (X_t) and could be detected according to the detection probability curve during EGD screening.

Tumor growth was modeled as an increase according to a sigmoid curve; the maximum diameter of the tumor (X_m) was determined from the maximum tumor diameter found in the cohort. This sigmoid curve was determined by defining the following sigmoid function to best fit the individual tumors found in the cohort:

$$f(t, X_m, k, x_o) = S\frac{1}{1 + \exp(-k \times (t - x_o))}$$

where x_0 indicated the point at which the tumor is half its maximum size.

The constructed model outputs the number of tumors detected, the interval between tumor occurrence and detection, tumor size at detection, and the tumor depth (deep SM invasion or not). The HpNGN detection rate was calculated as:

$$HpNGN\ detection\ rate = \frac{The\ number\ of\ detected\ HpNGN}{The\ number\ of\ generated\ HpNGN\ in\ the\ cohort}$$

Strategies and outcome measurement

The screening efficiencies of the different EGD screening strategies were compared using a simulation model. The screening start ages were 40, 45, and 50 years, and the screening end age was fixed at 70 years. The screening intervals were 2, 5, and 10 years. A number-needed-to-test (NNT) analysis was used to compare the nine strategies. The NNT was calculated using the following formula, as previously reported [26]: the lower the number was, the more efficient the strategy was.

$$NNT = \frac{The\ total\ number\ of\ EGD\ performed\ in\ the\ cohort}{The\ number\ of\ HpNGN\ cases\ detected\ in\ the\ strategy}$$

Statistical analyses and modeling

All statistical analyses were performed using R software 4.0.4. Mathematical modeling was performed using Python software 3.10.12. Tumors were randomly generated by time and phase using a random number algorithm based on a pre-determined tumor prevalence per generation. A linear regression model was used to predict the deep SM invasion rate of HpNGNs.

Results

Baseline characteristics of patients with HpNGNs

In total, 519,368 EGDs were included in the analysis (Supplementary Fig. 4). HpNGNs were detected in 108 patients with 113 lesions (0.021%). Of these, tumor characteristics were analyzed in 34 PSRCC, 26 GA-FG, 30 FGA-raspberry type, and seven undifferentiated-type cases for constructing the simulation model. Previous EGD was performed in 26 (76.5%), 23 (88.5%), 23 (76.7%), and 6 (85.7%) patients,

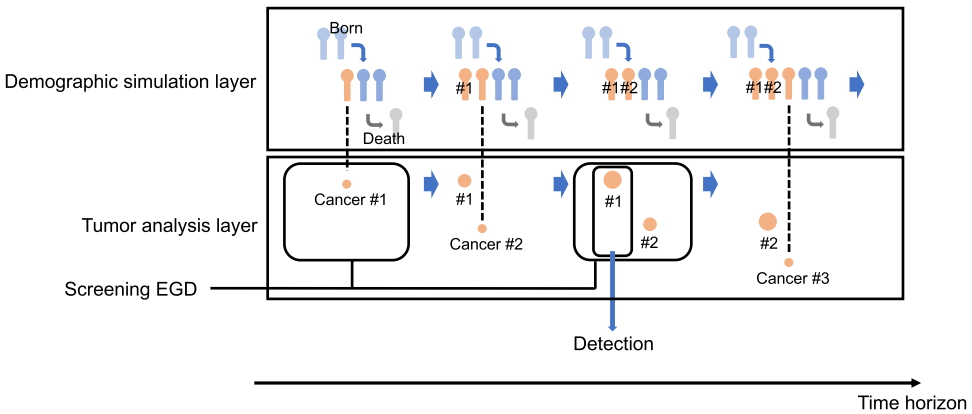

Fig. 1 Scheme of the mathematical simulation model. This model consists of the demographic simulation and tumor analysis layers. Regarding the demographic simulation layer, annual demographic change can be simulated using a predefined birth rate and mortality. In this layer, cancers are generated along with the age-related prevalence. Considering the tumor analysis layer, the growth process of the generated cancer can be simulated using predefined tumor growth speed criteria. The cancer detection rate can be calculated based on the detection threshold size, missing rate, screening starting age, and screening interval

respectively. Of these, 12 (46.1%), 15 (65.2%), 13 (56.5%), and 1 (16.7%) underwent EGDs that could identify the lesions. Tumor growth rate (X_t), tumor detection threshold (X_{th}), and missing rate (M_r) were calculated from these images (Table 1). Tumor growth speed (X_t) was faster for the undifferentiated type than for PSRCC, GA-FG, and the FGA-raspberry type (11.3 mm/year, 2.5 mm/year, 2.7 mm/year, and 1.2 mm/year, respectively). The tumor detection threshold (X_{th}) was larger for the undifferentiated type than for the other HpNGNs (15.6 mm, 6.7 mm, 8.2 mm, and 3.6 mm, respectively). Next, the sigmoid function that best fitted the growth rate of the individual tumors found in the cohort was determined. The results differed significantly according to histopathological type (Supplementary Fig. 5). Finally, the detection probability by size was modeled using a similar sigmoid function based on the size of tumors at detection and missing rate (M_r). The detection probability of the undifferentiated type did not increase with increasing size in comparison with other HpNGNs (Supplementary Fig. 6).

HpNGN detection rate

A mathematical simulation model was constructed using a variable set based on the cohort data. Tumor occurrence, growth, and detection were simulated in 346,5836 individuals over a 70-year follow-up period. At 70 years of age without screening using EGD, the size of all HpNGNs occurring in the simulation cohort was calculated; the percentage of HpNGNs exceeding the pre-determined tumor detection threshold size was calculated to be 49.7% (approximately 50%). Based on the result, a screening strategy is considered less significant if it cannot achieve at least a 50% detection rate. The earlier the age at which screening began and the shorter the screening interval was, the higher the overall HpNGN detection rate (Fig. 2 and Supplementary Table 2) was. Analysis by histopathological type revealed that PSRCC, FGA-raspberry type, and undifferentiated type showed similar trends. However, no relationship was observed between the starting age of screening or interval and detection rate of GA-FG (Fig. 3 and Supplementary Table 2).

NNT analysis

The NNT used to detect HpNGNs varied widely among strategies as shown in Fig. 2. The NNT decreased with a later starting age of screening and longer screening intervals. Among the strategies for achieving a detection rate of at least 50% for the HpNGNs in the cohort, the strategy with the lowest NNT was EGD every 5 years, starting at 45 years of age (Fig. 2). This strategy also achieved a detection rate of more than 50% for PSRCC, FGA-raspberry type; undifferentiated type and showed moderate NNT for all HpNGN types (Fig. 3).

Tumor size and deep SM invasion rate

Size and deep SM invasion rate of the HpNGNs at detection time were calculated for each strategy. All strategies detected the PSRCC, GA-FG, and FGA-raspberry types at sizes less than 20 mm, whereas undifferentiated tumors were identified at sizes more than 20 mm in some strategies (Fig. 4 and Supplementary Table 2). Regarding the strategy for screening every 5 years starting at 45 years of age, which is a superior strategy in terms of both detection rate and NNT, the tumor size was detected at < 20 mm for all histopathological types. The deep SM invasion rate was higher for the undifferentiated type than for GA-FG in all strategies (Fig. 5 and Supplementary Table 2). Adapting the strategy for screening every 5 years starting at 45 years of age, the deep SM invasion rate was 15.4% for GA-FG and 29.7% for the undifferentiated type.

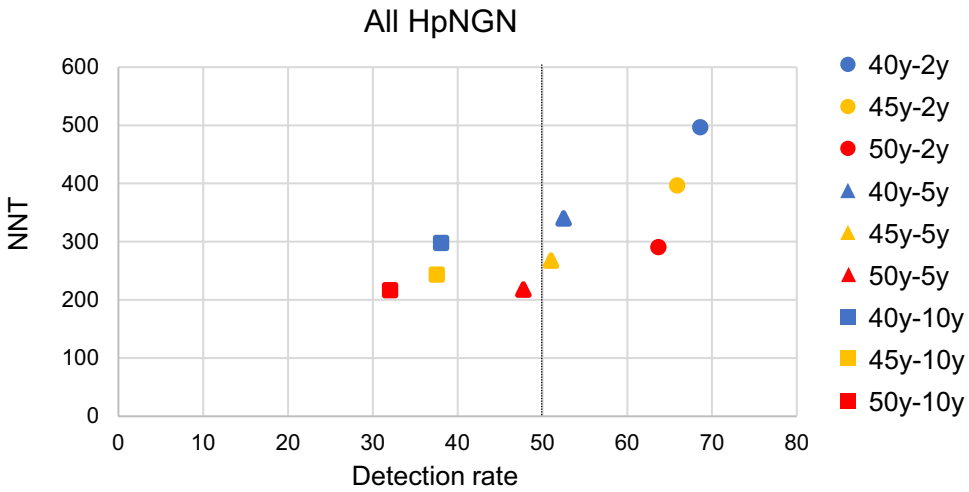

Fig. 2 Detection rate and number-needed-to-test (NNT) value of each screening strategy for the detection of *H. pylori*-naïve gastric neoplasms. Among the strategies that achieves a 50% detection rate, the screening strategy with a 5-year interval starting at 45 years of age has the lowest NNT

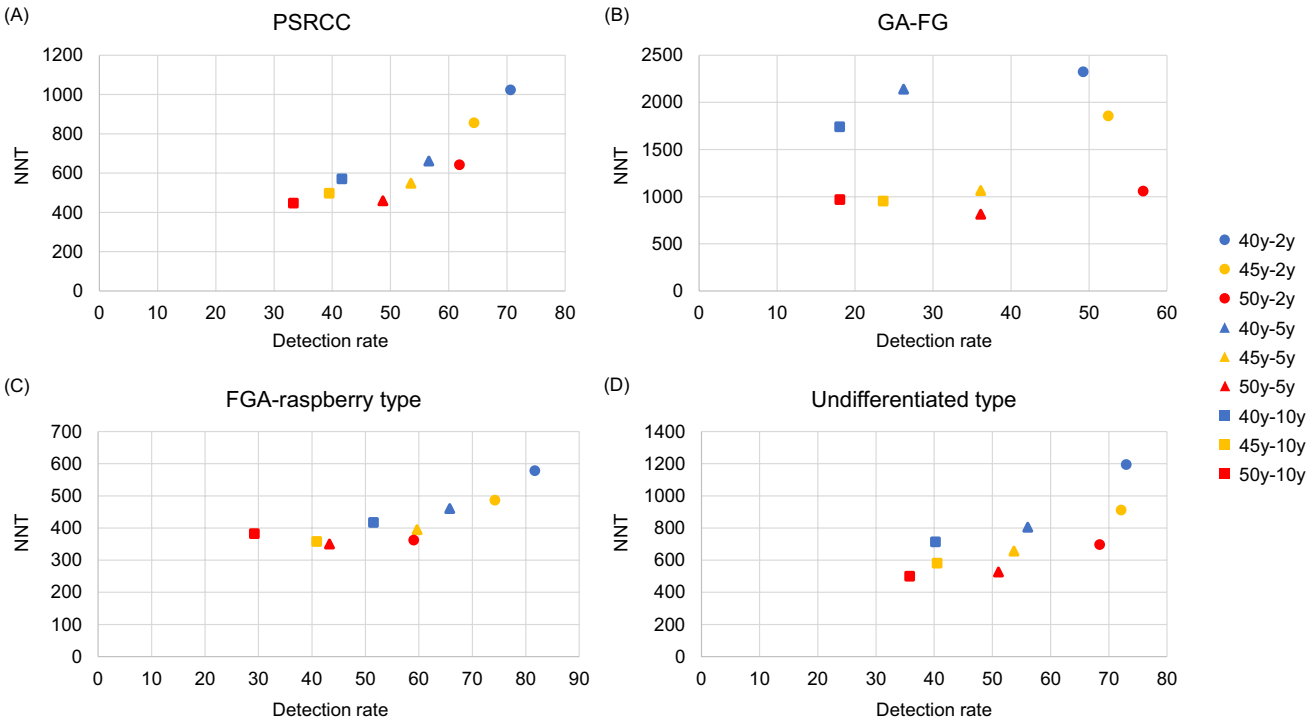

Fig. 3 Detection rate and number-needed-to-test (NNT) value of each screening strategy for the detection of **A** pure signet ring cell carcinoma (PSRCC), **B** gastric adenocarcinoma of the fundic gland type (GA-FG), **C** foveolar gastric adenoma-raspberry type (FGA-raspberry type), and **D** undifferentiated-type cancer

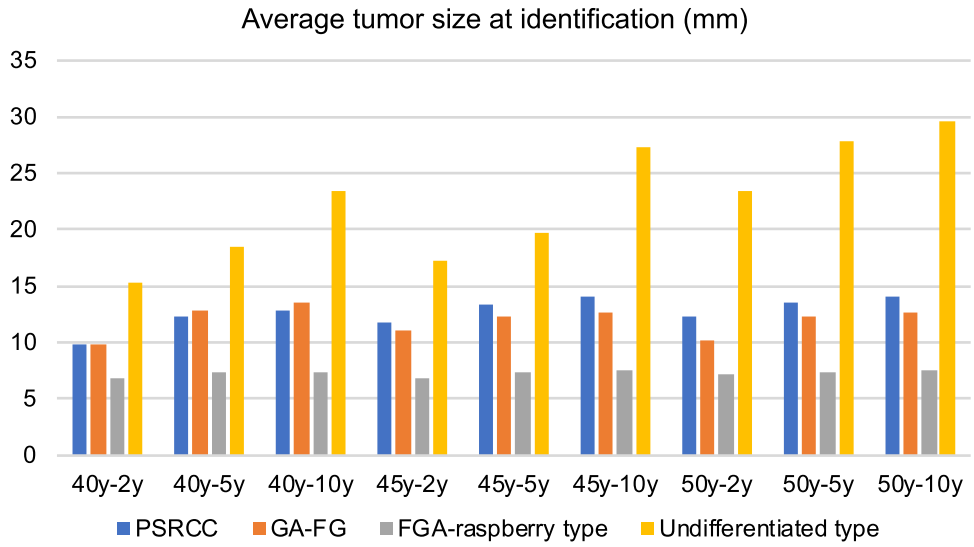

Fig. 4 Average tumor size at identification (mm) for each screening strategy. Pure signet ring cell carcinoma (PSRCC), gastric adenocarcinoma of the fundic gland type (GA-FG), and foveolar gastric adenoma-raspberry type (FGA-raspberry type) are identified at a small size (< 20 mm) in all strategies. In contrast, undifferentiated-type cancer is identified in a much larger size. Adopting the screening strategy with a 5-year interval starting at 45 years of age, undifferentiated-type cancers were identified at an average size of less than 20 mm

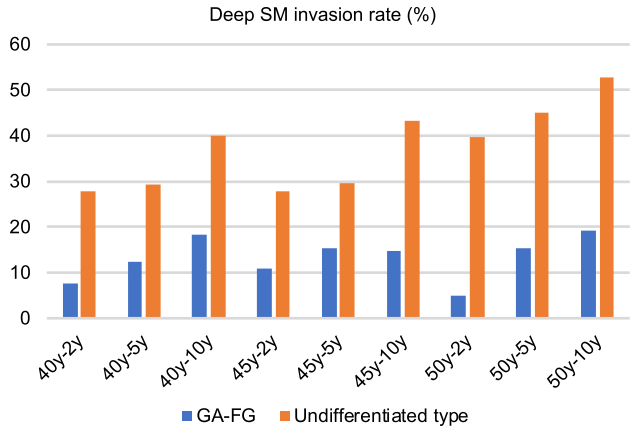

Fig. 5 Deep submucosa (SM) invasion rate of gastric adenocarcinoma of the fundic gland type (GA-FG) and undifferentiated-type cancer for each strategy. Adopting the screening strategy with a 5-year interval starting at 45 years of age, the deep SM invasion rate is less than 30% when undifferentiated-type cancer is detected

Discussion

In Japan, population-based GC screening has been an important public health theme for the past several decades due to the large number of GC-related deaths, which reflect a high *H. pylori*-positive rate. Although stomach screening with barium has been performed [27, 28], the effectiveness of EGD screening in GC has been proven [29–32]. Additionally, EGD use for population-based GC screening was approved in 2014 [33]. However, the usefulness of the same EGD screening strategy for the present era, when the incidence of HpRGCs has declined and the potential for HpNGNs occurrence has relatively increased, is unclear. EGD screening at a high frequency only for detecting rare diseases such as HpNGN is not recommended from a cost-effectiveness perspective. The simulation results showed that the screening strategy currently implemented in Japan as population-based screening every 2 years from age 50 was inferior to our recommended strategy (every 5 years from age 45) in terms of NNT. In future, with declining HPRGC prevalence, steering the project toward a strategy for detecting HpNGN with poor prognosis will be necessary, such as undifferentiated type cancer, while reducing the overall cost of the project by extending the intervals between EGDs rather than the traditional strategy. To our knowledge, this is the first study to discuss the screening strategy for detecting HpNGNs in terms of screening efficiency.

A major advantage of our mathematical simulation model is that it allowed us to establish cohorts that are more consistent with the real world. The age-specific incidence of HpNGN among 40- to 70-year-olds in the simulations was not significantly different from the prevalence underlying the simulations (Supplementary Table 3). Furthermore, the model could incorporate predefined tumor detection thresholds and missing rates as parameters while accurately reproducing the tumor growth process. The findings also indicated the importance of calculating the detection rate of tumors and determining tumor characteristics at detection time: size, time elapsed since occurrence, and deep SM invasion rate.

Most model-based simulation studies built their models by citing old data from previous reports or public databases and thus did not accurately reflect the most recent real-world trends [34, 35]. In this study, the model was constructed using a database with the most recent 6-year health checkup data from 12 Japanese facilities. Therefore, the data accurately reflected a cohort with a large number of *H. pylori*-uninfected individuals in an urban area of Japan, with minimal bias.

Detailed analysis of the simulation results showed that the detection rate was higher for strategies with a higher total number of EGDs (Supplementary Table 2) because the higher the number of EGDs was, the greater the chance was to detect a lesion in the subsequent EGD even if it was missed once. In addition, the detection rate was affected by the detection threshold size, missing rate, age at which the tumor was most likely to develop, and age at which screening was started. This was a complex interaction that would not result in identical detection rates across strategies.

The concept of screening for HpNGN is uncertain, and the optimal strategy may vary depending on the concept. In this study, we assumed that the most important aspect of EGD screening to detect HpNGN was early detection of lesions before they became invasive cancer. Particularly, we considered the undifferentiated type of HpNGN to be an important target for detection due to its poor prognosis. To evaluate whether the strategies determined as a result of the base case analysis could efficiently detect tumors before they developed into invasive cancer, a sensitivity analysis was performed by varying the detection rate threshold from 30 to 60%. The result showed that the optimal strategy varied greatly depending on the threshold. However, the deep SM invasion rate, particularly for the undifferentiated type with poor prognosis, was the lowest at a threshold of 50% (Supplementary Table 4). This indicated that even with a strategy targeting all types of HpNGN, detecting undifferentiated types with a poor prognosis at an earlier stage was possible. However, recognizing that the optimal strategy choice might vary widely depending on the screening concept was important.

One topic of debate is the appropriate tumor detection rate that is acceptable for the sensitivity of the strategy. The sensitivity of the Japanese report validating the ability of annual EGD screening was 97.7% [27], whereas the Korean report of biennial EGD screening had a sensitivity of 69.3% [36]. However, since these studies considered EGD as the

gold standard and did not account for lesions that could not be diagnosed by EGD, these were not genuine sensitivity values. The detection rate used in this study was defined as the number of tumors found relative to the number of tumors that occurred, which is an indicator of true sensitivity. In this study, we assumed that if a 50% detection rate was achieved, the strategy would be acceptable for implementation. Among the strategies that achieved a 50% detection rate, the strategy with the lowest NNT, the most efficient strategy, was screening every 5 years starting at 45 years of age (Fig. 2).

This study has some limitations. First, the collected cohort data included *H. pylori*-positive and post-eradication cases. Therefore, although the HpNGN prevalence data employed to construct the model did not reflect the prevalence among *H. pylori*-uninfected cases, it reflected the prevalence of HpNGN among individuals who were screened for GC in Japan. Second, due to the low reliability of the collected data for the prevalence of HpNGN among individuals aged ≥ 70 years, the age of screening termination was set to 70 years in this study's simulations. Therefore, the effectiveness of this strategy in individuals aged over 70 years could not be confirmed. Third, the mathematical model used in this study did not allow the calculation of incremental cost-effectiveness ratios, which could be used as outcomes when using Markov models, complicating the comparison of the results with those of other simulation models. Fourth, the assumption that the tumor growth rate follows a sigmoid curve might not be accurate, since some types of HpNGNs could grow without limits. However, setting a tumor detection threshold size, this effect was avoided because almost 100% of the individual tumors were detected before they reached the maximum size set by the sigmoid curve. Fifth, since data on HPRGC during the study period was not collected, the prevalence of HpRGC and HpNGC could not be compared. Finally, parameters, such as tumor growth rate and detection threshold size, may be inaccurate with small cohort data. Particularly, only six undifferentiated lesions were used for measurements. Additionally, although this study assumed the same growth pattern for each type of HpNGN, the actual tumor growth rates may not be the same. More accurate modeling studies with larger datasets should be performed in future to confirm the robustness of this study.

Conclusions

A mathematical simulation model built on the most recent six years of multicenter cohort data determined that the optimal strategy for detecting HpNGNs was screening every 5 years starting at 45 years of age under the concept of detecting HpNGNs at an earlier stage. Using this strategy, most HpNGNs, including undifferentiated-type GCs, were found to have an average size of less than 20 mm and deep SM invasion rate of less than 30%. Novel mathematical modeling techniques may be useful for screening optimization in future studies.

Supplementary Information The online version contains supplementary material available at https://doi.org/10.1007/s10120-024-01525-2.

Author contributions FI and KO designed the study. FI, YT, TH, TK, KM, YY, CY, YH, SO, KU, YM, HN, HU, MK, YT, and YM acquired data. FI and KM processed data. FI and SS interpreted data. FI and KO performed the modeling analyses. SS supervised the study. FI prepared the manuscript.

Funding This study was supported by the JGCA Research Grant (JGCA-037) and Health, Labour and Welfare Sciences Research Grants (Research for Promotion of Cancer Control Programmes) (24EA0101).

Data availability Clinical data are available from the corresponding author upon request.

Declarations

Conflict of interest SS received honoraria for lectures from Fujifilm and Olympus Corporation. The other authors declare that they have no conflicts of interest.

References

1. Fukase K, Kato M, Kikuchi S, Inoue K, Uemura N, Okamoto S, et al. Effect of eradication of Helicobacter pylori on incidence of metachronous gastric carcinoma after endoscopic resection of early gastric cancer: an open-label, randomised controlled trial. Lancet. 2008;372:392–7.
2. Choi IJ, Kook M-C, Kim Y-I, Cho S-J, Lee JY, Kim CG, et al. Helicobacter pylori therapy for the prevention of metachronous gastric cancer. N Engl J Med. 2018;378:1085–95.
3. Nakata R, Nagami Y, Hashimoto A, Sakai T, Ominami M, Fukunaga S, et al. Successful eradication of *Helicobacter pylori* could prevent metachronous gastric cancer: a propensity matching analysis. Digestion. 2021;102:236–45.
4. Watari J, Tomita T, Tozawa K, Oshima T, Fukui H, Miwa H. Preventing metachronous gastric cancer after the endoscopic resection of gastric epithelial neoplasia: roles of *Helicobacter pylori* eradication and aspirin. Gut Liver. 2020;14:281–90.
5. Kwak HW, Choi IJ, Cho SJ, Lee JY, Kim CG, Kook MC, et al. Characteristics of gastric cancer according to *Helicobacter pylori* infection status. J Gastroenterol Hepatol. 2014;29:1671–7.
6. Na JH, Lee SY, Kim JH, Sung IK, Park HS. *Helicobacter pylori* infection status and gastric tumor incidence according to the year of birth. Gut Liver. 2024;18:457–64.
7. Yamada A, Kaise M, Inoshita N, Toba T, Nomura K, Kuribayashi Y, et al. Characterization of *Helicobacter pylori*-naïve early gastric cancers. Digestion. 2018;98:127–34.
8. Ishibashi F, Suzuki S, Nagai M, Mochida K, Morishita T. Optimizing *Helicobacter pylori* treatment: an updated review of empirical and susceptibility test-based treatments. Gut Liver. 2023;17:684–97.
9. Kotani S, Shibagaki K, Hirahara N, Hasegawa N, Tanabe R, Ebisutani Y, et al. Clinicopathologic differences of gastric neoplasms

between *Helicobacter pylori*-infected and -naïve patients: a multicenter retrospective analysis. J Gastroenterol. 2024;59:1–10.
10. Ishibashi F, Hirasawa T, Ueyama H, Minato Y, Suzuki S. Exploring quality indicators for the detection of *Helicobacter pylori*-naïve gastric cancer: a cross-sectional nationwide survey. Clin Endosc. 2023;56:460–9.
11. Ishibashi F, Kobayashi K, Kawakami T, Tanaka R, Sugihara K, Baba S. Quality management system for screening esophagogastroduodenoscopy improves detection of *Helicobacter pylori* -negative interval gastric cancer. Endosc Int Open. 2021;9:E1900–8.
12. Ishibashi F, Kobayashi K, Fukushima K, Tanaka R, Kawakami T, Kato J, et al. Quality indicators for the detection of *Helicobacter pylori*-negative early gastric cancer: a retrospective observational study. Clin Endosc. 2020;53:698–704.
13. Ueyama H, Yao T, Nakashima Y, Hirakawa K, Oshiro Y, Hirahashi M, et al. Gastric adenocarcinoma of fundic gland type (chief cell predominant type): proposal for a new entity of gastric adenocarcinoma. Am J Surg Pathol. 2010;34:609–19.
14. Ueyama H, Matsumoto K, Nagahara A, Hayashi T, Yao T, Watanabe S. Gastric adenocarcinoma of the fundic gland type (chief cell predominant type). Endoscopy. 2014;46:153–7.
15. Ueyama H, Yao T, Akazawa Y, Hayashi T, Kurahara K, Oshiro Y, et al. Gastric epithelial neoplasm of fundic-gland mucosa lineage: proposal for a new classification in association with gastric adenocarcinoma of fundic-gland type. J Gastroenterol. 2021;56:814–28.
16. Ishibashi F, Fukushima K, Ito T, Kobayashi K, Tanaka R, Onizuka R. Influence of *Helicobacter pylori* infection on endoscopic findings of gastric adenocarcinoma of the fundic gland type. J Gastric Cancer. 2019;19:225–33.
17. Shibagaki K, Fukuyama C, Mikami H, Izumi D, Yamashita N, Mishiro T, et al. Gastric foveolar-type adenomas endoscopically showing a raspberry-like appearance in the *Helicobacter pylori* -uninfected stomach. Endosc Int Open. 2019;7:E784–91.
18. Shibagaki K, Ishimura N, Kotani S, Fukuyama C, Takahashi Y, Kishimoto K, et al. Endoscopic differential diagnosis between foveolar-type gastric adenoma and gastric hyperplastic polyps in *Helicobacter pylori*-naïve patients. Gastric Cancer. 2023;26:1002–11.
19. Horiuchi Y, Hirasawa T, Fujisaki J. Endoscopic features of undifferentiated-type early gastric cancer in patients with *Helicobacter pylori*-uninfected or -eradicated stomachs: a comprehensive review. Gut Liver. 2024;18:209–17.
20. Nikaido M, Kakiuchi N, Miyamoto S, Hirano T, Takeuchi Y, Funakoshi T, et al. Indolent feature of *Helicobacter pylori*-uninfected intramucosal signet ring cell carcinomas with CDH1 mutations. Gastric Cancer. 2021;24:1102–14.
21. Cho SY, Park JW, Liu Y, Park YS, Kim JH, Yang H, et al. Sporadic early-onset diffuse gastric cancers have high frequency of somatic CDH1 alterations, but low frequency of somatic RHOA mutations compared with late-onset cancers. Gastroenterology. 2017;153:536-549.e26.
22. Kiso M, Urabe Y, Ito M, Masuda K, Boda T, Kotachi T, et al. Clinical and genomic characteristics of mucosal signet-ring cell carcinoma in *Helicobacter pylori*-uninfected stomach. BMC Gastroenterol. 2020;20:243.
23. Funakoshi T, Miyamoto S, Kakiuchi N, Nikaido M, Setoyama T, Yokoyama A, et al. Genetic analysis of a case of *Helicobacter pylori*-uninfected intramucosal gastric cancer in a family with hereditary diffuse gastric cancer. Gastric Cancer. 2019;22:892–8.
24. Horiuchi Y, Fujisaki J, Ishizuka N, Omae M, Ishiyama A, Yoshio T, et al. Study on clinical factors involved in *Helicobacter pylori*-uninfected, undifferentiated-type early gastric cancer. Digestion. 2017;96:213–9.
25. Gastric J. Cancer association. Japanese classification of gastric carcinoma: 3rd English edition. Gastric Cancer. 2011;14(2):101–12.
26. Ishibashi F, Suzuki S, Kobayashi K, Tanaka R, Kawakami T, Mochida K, Nagai M, Ishibashi Y, Morishita T. Cost-effectiveness analysis of single colonoscopy versus single fecal test for colorectal cancer diagnosis and treatment. J Gastroenterol Hepatol. 2024. https://doi.org/10.1111/jgh.16509.
27. Hamashima C, Ogoshi K, Okamoto M, Shabana M, Kishimoto T, Fukao A. A community-based, case-control study evaluating mortality reduction from gastric cancer by endoscopic screening in Japan. PLoS ONE. 2013;8:e79088.
28. Hamashima C, Shabana M, Okada K, Okamoto M, Osaki Y. Mortality reduction from gastric cancer by endoscopic and radiographic screening. Cancer Sci. 2015;106:1744–9.
29. Jun JK, Choi KS, Lee H-Y, Suh M, Park B, Song SH, et al. Effectiveness of the Korean national cancer screening program in reducing gastric cancer mortality. Gastroenterology. 2017;152:1319-28.e7.
30. Noh C-K, Lee E, Lee GH, Kang JK, Lim SG, Park B, et al. Association of intensive endoscopic screening burden with gastric cancer detection. JAMA Netw Open. 2021;4:e2032542.
31. Kusano C, Gotoda T, Ishikawa H, Suzuki S, Ikehara H, Matsuyama Y. Gastric cancer detection rates using gastrointestinal endoscopy with serological risk stratification: a randomized controlled trial. Gastrointest Endosc. 2024. https://doi.org/10.1016/j.gie.2024.01.022.
32. Gotoda T, Ishikawa H, Kusano C, Suzuki S, Ohnishi H, Sugano K, et al. Randomized controlled trial comparing the costs of gastric cancer screening systems between serological risk-based upper gastrointestinal endoscopy and the existing barium photofluorography: gastric cancer screening labeled by serum examination in place of aged gastric cancer organized screening systems (GALAPAGOS study). Gastric Cancer. 2024;27:36–48.
33. Mabe K, Inoue K, Kamada T, Kato K, Kato M, Haruma K. Endoscopic screening for gastric cancer in Japan: current status and future perspectives. Dig Endosc. 2022;34:412–9.
34. Kowada A. A population-based *Helicobacter pylori* eradication strategy is more cost-effective than endoscopic screening. Dig Dis Sci. 2023;68:1735–46.
35. Huang HL, Leung CY, Saito E, Katanoda K, Hur C, Kong CY, et al. Effect and cost-effectiveness of national gastric cancer screening in Japan: a microsimulation modeling study. BMC Med. 2020;18:257.
36. Ryu JE, Choi E, Lee K, Jun JK, Suh M, Jung KW, et al. Trends in the performance of the Korean National Cancer Screening Program for gastric cancer from 2007 to 2016. Cancer Res Treat. 2022;54:842–9.

Authors and Affiliations

Fumiaki Ishibashi[1] · Kosuke Okusa[2] · Yoshitaka Tokai[3] · Toshiaki Hirasawa[3] · Tomohiro Kawakami[4] · Kentaro Mochida[1,4] · Yuka Yanai[5] · Chizu Yokoi[5] · Yuko Hayashi[6] · Shun-ichiro Ozawa[7] · Koji Uraushihara[8] · Yohei Minato[9] · Hiroyuki Nakanishi[10] · Hiroya Ueyama[11] · Mikinori Kataoka[12] · Yuzo Toyama[13] · Yuji Mizokami[14] · Sho Suzuki[1]

✉ Fumiaki Ishibashi
ishibashi-gast@iuhw.ac.jp

1 Department of Gastroenterology, International University of Health and Welfare Ichikawa Hospital, 6-1-14, Konodai, Ichikawa-shi, Chiba 272-0827, Japan

2 Faculty of Science and Engineering, Department of Data Science for Business Innovation, Chuo University, Tokyo 112-8551, Japan

3 Department of Gastroenterology, Cancer Institute Hospital, Tokyo 135-8550, Japan

4 Koganei Tsurukame Clinic, Endoscopy Center, Tokyo 184-0004, Japan

5 National Center for Global Health and Medicine, Department of Gastroenterology, Tokyo 162-8655, Japan

6 National Center for Global Health and Medicine, Department of Medical Examination Center, Tokyo 162-8655, Japan

7 Department of Gastroenterology and Hepatology, Japan Community Health Care Organization Yamanashi Hospital, Yamanashi 400-0025, Japan

8 Department of Gastroenterology, Showa General Hospital, Tokyo 187-8510, Japan

9 Department of Gastrointestinal Endoscopy, NTT Medical Center Tokyo, Tokyo 141-8625, Japan

10 Department of Gastroenterology and Hepatology, Musashino Red Cross Hospital, Tokyo 180-8610, Japan

11 Department of Gastroenterology, Juntendo University School of Medicine, Tokyo 113-8431, Japan

12 Department of Gastroenterology, International University of Health and Welfare Mita Hospital, Tokyo 108-8239, Japan

13 Department of Gastroenterology, New Tokyo Hospital, Chiba 270-2232, Japan

14 Department of Medical Examination Center, New Tokyo Hospital, Chiba 270-2232, Japan